Perturbed ac Stark Effect for Attosecond Optical-Waveform Sampling

Kang Mi,[1] Wei Cao,[1,*] Huiyao Xu,[1] Yunlong Mo,[1] Zhen Yang,[1] Pengfei Lan,[1] Qingbin Zhang,[1,†] and Peixiang Lu[1,2,‡]

[1]*School of Physics and Wuhan National Laboratory for Optoelectronics, Huazhong University of Science and Technology, Wuhan 430074, China*

[2]*Hubei Key Laboratory of Optical Information and Pattern Recognition, Wuhan Institute of Technology, Wuhan 430205, China*

We demonstrate an all-optical method for time-domain characterization of ultrashort optical pulses using nonionizing lasers. A moderately intense laser pulse couples the doubly excited states of helium and induces the ac Stark effect. A synchronized weak signal field perturbs the coupling process and alters the quasienergies of the dressed atom, upon which the carrier oscillation of the signal field is encoded. The nonionizing lasers used in current approach minimize plasma-induced pulse distortion and provide a complementary detection scheme for effective and reliable optical oscilloscope.

I. INTRODUCTION

The development of femtosecond pulses together with the attosecond pulses produced by them makes it possible for one to go into detail about the electron dynamics of atoms, molecules, and solids [1,2]. Nowadays, most ultrafast optics laboratories have the ability to generate ultrashort near-infrared (NIR) laser pulses, the electric fields of which only oscillate four or five times during the whole pulse duration. Therefore, their temporal structure is crucial for the detection and control of electron dynamics [3–6].

However, the upper limit of the sampling frequency of modern detectors based on electronics is of the order of gigahertz due to the limitations of their working principle [7] and many approaches have been developed to diagnose the temporal structure of optical pulses. The simplest autocorrelation method only gives limited information about the pulse envelope [8]. Frequency-domain measurements are most commonly used for broadband pulse characterization, including frequency-resolved optical gating (FROG) [9], spectral-phase interferometry for direct electric field reconstruction (SPIDER) [10], and all their variants [11, 12]. But these methods require all the reflecting and transmitting optical components to have ultrabroad bandwidths and at the same time large phase-matching bandwidths of the nonlinear medium are needed. The dispersion-scan

(*d*-scan) technique can be performed with more simplified devices compared to FROG and SPIDER, but it relies on complicated reconstruction algorithms [13,14]. With the invention of high-harmonic-based attosecond pulses, direct time-domain measurement of the electric field of an optical pulse becomes possible. Photoelectron spectroscopy such as the attosecond streak camera is a reliable way of directly measuring the vector potential of the electric field [15–17]. Compared to all-optical approaches, it normally requires sophisticated particle-detection techniques and the data acquisition can be time consuming in order to avoid the space-charge effect. Recently, all-optical approaches based on perturbed high-harmonic generation (HHG) have been demonstrated to successfully reconstruct the waveform of an optical pulse [18–21]. However, HHG is a strong-field process accompanied by laser-driven plasma, which may distort the waveform of the electric field that passes through [22,23]. Thus care has to be taken to minimize this propagation effect on the signal pulse that is to be measured.

Here, we demonstrate an all-optical method for direct time-domain measurement of the electric field oscillations based on the EUV absorption spectrum of laser-dressed atoms. The current scheme utilizes nonionizing lasers to induce the ac Stark effect in the helium atom. By interrogating the quasienergies of the laser-dressed atom using EUV attosecond pulses, the waveform of an optical pulse can be precisely diagnosed. The nonionizing lasers used in the current approach minimize the plasma-induced pulse distortion that is generally encountered in strong-field-based schemes, providing a reliable approach for waveform sampling in the optical domain.

*weicao@hust.edu.cn

†zhangqingbin@hust.edu.cn

‡lupeixiang@mail.hust.edu.cn

II. PRINCIPLE OF OPTICAL-WAVEFORM SAMPLING

Figure 1 shows the principle of the time-domain waveform-sampling method. A moderately intense driving pulse (DP) couples the energy levels and induces the ac Stark effect in the $N = 2$ Rydberg series of helium atoms. When the coupling condition is resonant, where the frequency of the laser field coincides with a two-level transition, each individual energy of the bare atom splits into two components, this being known as Autler-Townes (AT) splitting [24]. When the coupling is nonresonant, the energies of the bare atom experience a shift, termed the ac Stark
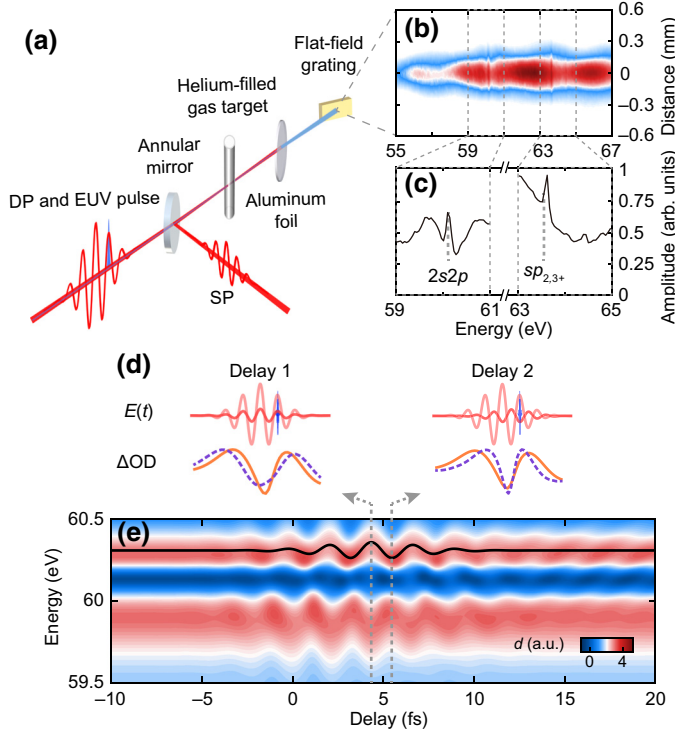

FIG. 1. A schematic diagram of the optical-waveform-sampling method. (a) The experiment is using a three-pulse configuration. The EUV pulse is phase locked with the DP. The SP is combined with the DP using an annular mirror and delayed by a high-precision delay stage. All three pulses are copropagating and are focused into a helium-filled gas target. The absorption spectrum is analyzed with an EUV spectrometer. (b) A typical two-dimensional (2D) EUV spectrum taken using a charged-coupled device (CCD) camera and (c) the spectrum lineout by integrating the vertical axis, while the gray dashed lines represent the energies of the undressed $2s2p$ and $sp_{2,3+}$ states. (d) Without the perturbing SP, the helium $2s2p$ shows an AT-splitting absorption profile (solid lines). When a relatively weak SP is introduced, the AT-splitting feature is perturbed and depends sensitively on the arrival time of the signal pulse (dashed lines). (e) A simulated helium $2s2p$ transient absorption spectrogram using the few-level model. The energy shift of the individual AT-splitting peak resembles the incident SP waveform (black solid line).

shift [25]. These aforementioned laser-dressed atomic levels are detectable when a broadband EUV attosecond pulse or attosecond pulse train is illuminated on the laser-atom combined system [4,26]. Figure 1(b) shows the typical transmitted EUV spectrum of a helium atom dressed by the NIR field. The bifurcation of the $2s2p$ peak around 60 eV results from the near-resonant laser coupling between the $2s2p$ and $2p^2$ states and is a typical AT-splitting feature. Other high-lying bright states above 63 eV are off resonance with any intermediate dark states and thus mainly experience the nonresonant ac Stark shift. As is demonstrated by Chini *et al.*, the transient absorption spectrum can successfully capture the subcycle ac-Stark-shifted energy, i.e., the transient quasienergy of the dressed atom, when the EUV attosecond pulse is phase locked with the DP [26]. In this case, the EUV pulse is acting as a fast probe to access the instantaneous intensity of the dressing field. In the single-NIR pulse configuration, the laser-induced energy shift is either proportional to the laser intensity (the ac Stark shift) or proportional to the envelope of the electric field of the NIR pulse (AT splitting). None of these absorption features shows clear correspondence to the oscillating electric field of a laser pulse. Therefore, the regular attosecond transient absorption spectroscopy (ATAS) experiment using a single laser pulse is not suitable for direct time-domain sampling of an electric field. If an additional weak signal pulse (SP) is introduced to overlap with the DP, it perturbs the waveform of the DP slightly and induces an observable shift of the quasienergies, as shown schematically in Fig. 1(d). The position of the shifted quasienergy depends sensitively on the relative delay between the SP and the DP-EUV pulse pair. According to our theoretical derivation, for both resonant and nonresonant coupling conditions, the delay-dependent energy shift induced by the SP can be written as follows (for further details, see the Supplemental Material [27–30])

$$\delta E(\tau) \propto \mathcal{E}_2(t_0 - \tau) \cos\left[\omega_2(t_0 - \tau) + s(t_0 - \tau) - \phi_0\right]. \tag{1}$$

The incident SP electric field is $\mathcal{E}_2(t) \cos\left[\omega_2 t + s(t)\right]$, with $\mathcal{E}_2(t)$, ω_2 and $s(t)$ representing the time-dependent envelope, the central frequency, and the arbitrary temporal phase, respectively. t_0 is a time offset with respect to the peak of the DP and is mainly determined by the envelope of the DP [27]. Equation (1) indicates that the energy shift induced by the SP is a direct mapping of the waveform of the SP, except that an artificial phase offset $\phi_0 = \omega_1 t_0$ is introduced, where ω_1 is the central frequency of the DP. To confirm the validity of Eq. (1), we perform a numerical simulation using a few-level model incorporating the autoionizing process in helium doubly excited states [4]. The calculated results show that the shifted quasienergy has an excellent resemblance to the waveform of the signal

pulse, indicating a proof-of-principle demonstration of an optical oscilloscope using a nonionizing laser field.

III. RESULTS

A. Sampling experiments

The experiment is carried out using a three-pulse configuration as shown in Fig. 1(a). The NIR pulse produced by a 25-fs 800-nm titanium:sapphire amplifier is sent into a neon-filled hollow-core fiber for spectral broadening (span from 550 nm to 950 nm) and is compressed down to 7 fs using broadband chirped mirrors. A broadband 50:50 beam splitter splits the few-cycle laser pulse. The transmitted beam is then used to produce an EUV pulse via HHG. Temporally, the EUV pulse is a pulse-train structure consisting of several equally spaced attosecond bursts. The residual laser pulse copropagating with the EUV pulse is acting as the DP. The reflected beam is acting as the weak SP and recombines with the DP-EUV pulse pair via an annular mirror. The DP and the EUV pulse are phase locked, while the relative time between the DP and the SP can be adjusted precisely by a piezoelectric transducer with attosecond precision. The three pulses are focused into the helium-filled gas target (gas pressure 26.2 mbar). The residual DP and SP are filtered out by an aluminum foil. The EUV spectrum is analyzed with a high-resolution spectrometer that is composed of a flat-field grating and a CCD camera.

The experimental results are presented in Fig. 2. For each delay, the spectrum is accumulated for 1500 laser shots. The relative optical density (ΔOD) is evaluated from the measured spectra following the method in [31]. A reference spectrum is obtained by low-pass Fourier filtering the transmitted spectra. In this way the calculated absorption cross section represents the absorption with respect to the non-resonant continuum background. This reduced presentation of the absorption is enough for this optical-wave-sampling experiment, because the continuum absorption background has a negligible effect on the position of absorption or emission peaks. The delay step size is 400 as and is sufficient to sample the oscillation pattern of the SP with an approximately 700-nm central wavelength (with an approximately 2.4-fs period).

To get a visible splitting of the $2s2p$ state, we adjust the intensity of the DP to about 3×10^{12} W/cm^2, leading to a splitting of about 0.3 eV. The intensity of the SP is required to be much weaker than that of the DP to make the shifts of the energy levels proportional to the electric field of the SP. If the SP intensity is too high, i.e., comparable to the DP intensity, the higher-order term proportional to the intensity of the SP will be non-negligible and the energy shift can no longer correctly reflect the waveform of the SP [27]. In addition, the quantum-interference fringes due to multipath interference will be more profound, hindering the correct reconstruction of the SP electric field. On the
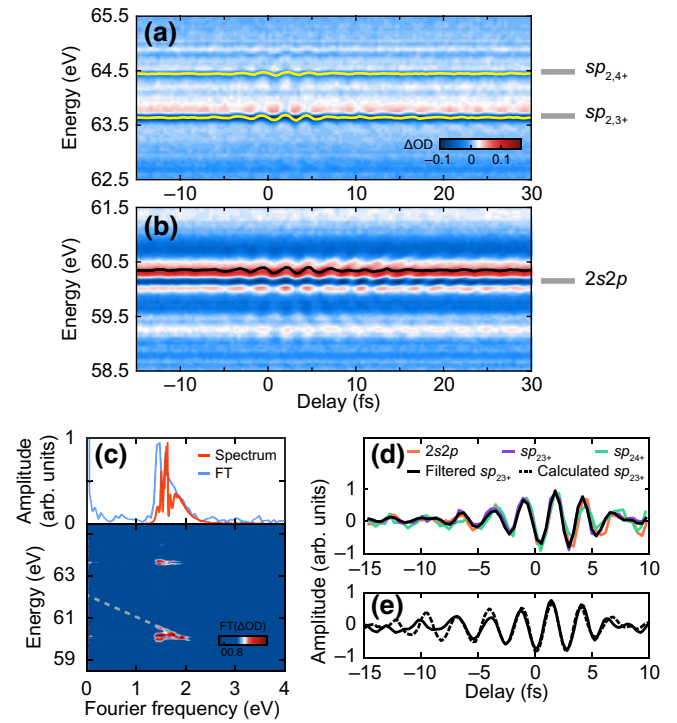

FIG. 2. The experimental results and analysis. (a),(b) The relative optical density (ΔOD) of the EUV pulse as a function of the time delay for two different photon-energy ranges corresponding to the ac Stark shift of $sp_{2,n+}$ ($n = 3, 4 \ldots$) states (a) and AT splitting of the $2s2p$ state (b). A positive delay means that the EUV pulse is preceding the SP. The black line is the centroid of the $2s2p$ upper-splitting absorption structure and the yellow lines represent the position of the laser-dressed $sp_{2,n+}$ states. (c) The Fourier transform (FT) of the transient absorption spectrogram along the delay axis. The red curve at the top is the experimentally measured SP spectrum. The blue curve is the Fourier-transform lineout integrated from 63.48 to 63.89 eV of the 2D FT spectrogram. (d) The extracted center of the $2s2p$ upper-splitting structure, $sp_{2,3+}$, $sp_{2,4+}$, and filtered $sp_{2,3+}$. (e) The retrieved SP waveform from the laser-dressed $sp_{2,3+}$ energy when the SP is overcompensated with 0.4 mm of fused silica (solid line) and the calculated waveform.

other hand, the SP should be intense enough for an accessible signal-to-noise ratio. Considering these, the intensity of the SP is set to be approximately 2×10^{11} W/cm^2. The energies of the $sp_{2,3+}$ and $sp_{2,4+}$ states oscillate with a time delay within the SP duration—even oscillation of the $sp_{2,5+}$ state can be observed [Fig. 2(a)]. The absorption feature corresponding to the $2s2p$ state splits into two parts and the energy of the upper part oscillates with a time delay [Fig. 2(b)]. The oscillations of the positions of the quasienergies observed in Figs. 2(a) and 2(b) have a common period of about 2.4 fs, corresponding to a roughly 700-nm central frequency, which is consistent with the measured spectrum of the SP. A hyperbolic line structure in the vicinity of the $2s2p$ absorption is clearly observed

for positive delays [Fig. 2(b)]. This is attributed to the multipath-interference phenomena [32–34].

Figure 2(c) shows the Fourier transform of Figs. 2(a) and 2(b) along the delay axis. The $2s2p$ and $sp_{2,3+}$ states have a Fourier frequency range from 1.4 to 2 eV. The dashed line in Fig. 2(c) intersects with the energy axis at 62.06 eV, which is the energy of the $2p^2$ state. This confirms that the hyperbolic line structure on the splitting structure of the $2s2p$ state in Fig. 2(b) indeed comes from the population transfer of the $2p^2$ state. The experimentally measured spectrum of the SP shows a good correlation with the Fourier frequency of the absorption peaks, as shown in Fig. 2(c). Figure 2(d) depicts the extracted energy oscillations of the $2s2p$ and $sp_{2,n+}$ ($n = 3, 4 \ldots$) states. The relative intensity of the upper and lower parts of the AT splitting is determined by the detuning of the DP wavelength with respect to the $2s2p$-$2p^2$ transition energy [34]. In the experiment, the upper part is stronger and possesses a better signal-to-noise ratio; therefore the upper part is chosen for analysis. All extracted oscillations possess a similar waveform, oscillating a few times within the main pulse duration. The extracted oscillations from high-lying Rydberg $sp_{2,n+}$ ($n = 3, 4 \ldots$) states are more reliable as compared to that of the $2s2p$ state by excluding the multipath-interference effect. A band-pass filter is used to select the frequency range of the SP spectrum from 500 nm to 1000 nm and the filtered energy oscillation of the $sp_{2,3+}$ state can most accurately reflect the electric field waveform of the SP. To further verify the validity of our sampling method, we change the waveform by reducing the thickness of the fused silica by 0.4 mm in the SP beam path, so that the signal pulse is elongated and carries a chirp. The calculated and measured waveforms are depicted in Fig. 2(e), which shows good agreement over the main part of the pulse duration. It should be noted that the laser that we use in the experiment is carrier-envelope-phase (CEP) unstabilized. Following the three-step model [35,36], the attosecond pulses are emitted at a specific phase of the driver due to its generation mechanism, i.e., the attosecond pulse is locked to the carrier of the driving field even though the CEP varies from laser shot to laser shot. This is actually essential for direct time-domain sampling of the oscillating carrier of the SP. Our numerical analysis shows that in case of a CEP-unstabilized laser, the current method can still precisely measure the carrier of the laser field, with the envelope information averaged (for further details, see the Supplemental Material [27,37]).

B. Simulations for AT splitting

To test the generality of the current method, we investigate the perturbed AT splitting of the $2s2p$ state using the few-level model (for further details, see the Supplemental Material [27]) for a signal pulse with different waveforms. In the calculation, the central photon energy

of the DP is set to 1.97 eV in order to be slightly blue detuned to the $2s2p$-$2p^2$ transition energy. In this case, the simulated result shows an asymmetric AT-splitting structure, with the upper component more profound [Fig. 3(a)], which is similar to the experimentally observed absorption spectrogram in Fig. 2(b). The EUV attosecond pulses are synchronized with the electric field of the DP, as predicted by the three-step HHG model [35,36]. Considering the depletion of the ground state of argon during harmonic generation, the attosecond pulses are generated mainly at the leading edge of the driving pulse [38,39]. We perform the numerical simulation of attosecond pulses produced by the driving field. The simulation results show that the dominant attosecond peak is produced about an optical cycle before the peak of the driving field [27]. Therefore, for convenience, we assume that the EUV pulse arrives
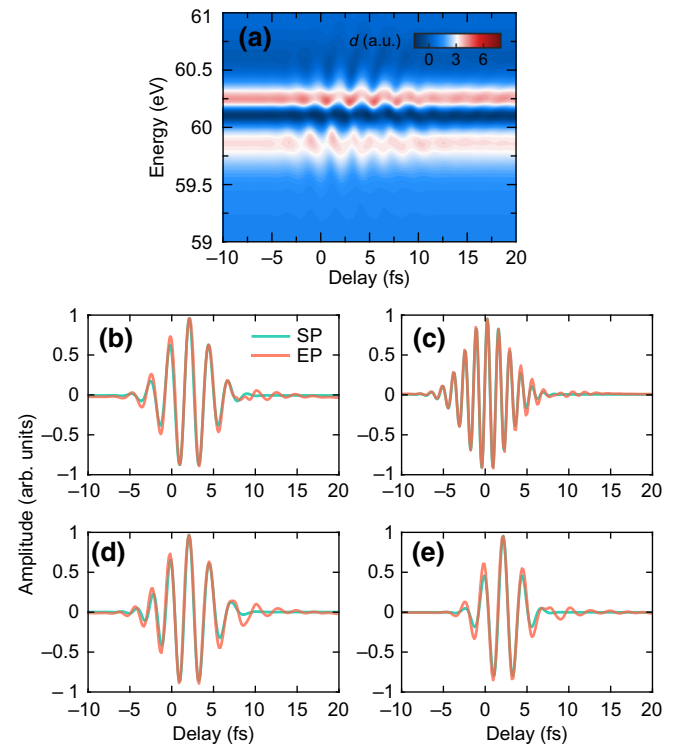

FIG. 3.   A few-level model simulation of the AT splitting. (a) a 2D transient absorption spectrogram, with the horizontal axis representing the delay between the SP and the DP. In the simulation, the EUV pulse arrives 2.5 fs before the DP and the 630-nm DP has a pulse duration of 6.5 fs and an intensity of 3×10^{12} W/cm^2. (b)–(e) Extracted pulses (EPs) by calculating the center of mass of the upper part of the AT-splitting structure (orange solid lines) as compared with the incident SPs (green solid lines) when different signal pulses are used. (b) The pulse duration of the SP is 4 fs and the central wavelength is 700 nm. (c) The pulse duration of the SP is 4 fs and the central wavelength is 400 nm. (d) Similar to (b) but with a temporal chirp. (e) The pulse duration of the SP is 3 fs and the central wavelength is 700 nm.

2.5 fs before the DP, to mimic the experimental conditions. Our numerical simulations also show that choosing values other than 2.5 fs does not affect the successful reconstruction of the waveform of the SP. Figures 3(b)–3(e) show the extracted oscillation of the central energy of the $2s2p$ absorption feature perturbed by the SP with four different waveforms. The central energy is obtained by calculating the weighted average of the upper part of the AT-splitting structure (from 60.1 eV to 60.7 eV). The good agreement between the extracted oscillation and the electric field of the SP indicates that the current scheme is a robust and reliable way of reconstructing a weak optical-signal pulse with arbitrary waveforms.

C. Simulations for the ac Stark shift

Both the analytical formula of Eq. (1) and the experimental measurement show that the absorption profiles of nonresonant Stark-shifted energy levels are also good candidates for waveform sampling. A two-electron time-dependent Schrödinger equation (TDSE) with reduced dimension is used to simulate the perturbed ac Stark shift of the helium $N = 2$ Rydberg series (for further details, see the Supplemental Material [27,40]). The model is already successfully used to get the absorption spectrum when the atom interacts with the combination of an EUV pulse and a NIR pulse in an attosecond pump-probe configuration [4]. The central wavelength of the DP is far from the resonant condition in the simulation; thus the doubly excited states manifold mainly undergoes the ac Stark shift. The results of the TDSE simulation are shown in Fig. 4. The oscillations of the $2s2p$, $sp_{2,3+}$, and $sp_{2,4+}$ energies are identical to the electric field of the original input signal pulse, proving the validity of the waveform-sampling method based on the perturbed nonresonant ac Stark shift.

IV. DISCUSSION

We demonstrate that ultrafast EUV absorption spectroscopy using nonionizing lasers can be used to perform direct time-domain measurement of the waveform of an ultrashort optical pulse. By tuning the atomic energy structure using the ac Stark effect and probing the quasienergy with an EUV absorption spectrum, the waveform of a petahertz electromagnetic field can be accurately detected. The validity of the method is verified by numerical simulations. Although the numerical analyses shown in Figs. 3 and 4 are carried out with an isolated attosecond pulse as a fast probe, the use of an attosecond pulse train instead should not alter the conclusion, due to the fact that the EUV pulse is a weak perturbative probe [4]. Our calculation confirms that the waveform-sampling method is still feasible when an EUV attosecond pulse train is utilized (see the Supplemental Material [27]), therefore providing a reliable approach to the development of an optical oscilloscope. It is worth noting that small oscillations still exist and persist for a much longer duration in the extracted waveform, as shown in Fig. 3. This is due to the laser-induced $2p^2$-to-$2s2p$ population transfer and is the main error of the current method. This error can be potentially eliminated by using a noncollinear geometry, in which the SP intersects with the DP at a small angle and the population-transfer-induced wave-mixing signal travels in a different direction compared to the EUV pulse [41]. This will also be the focus of future work in order to improve the waveform-sampling method presented here.
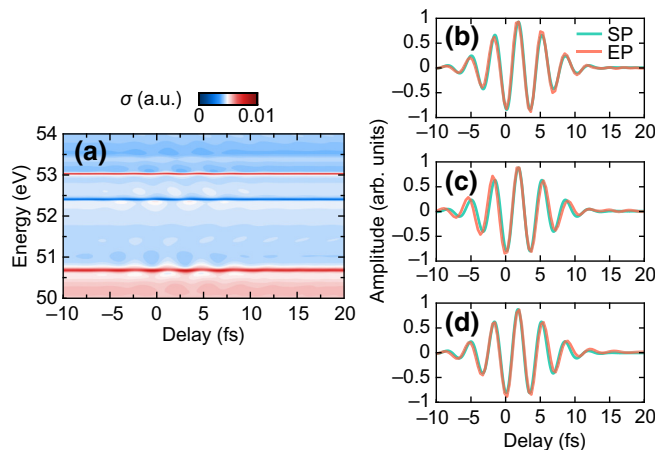
FIG. 4. The results of the two-electron TDSE model simulation for the ac Stark shift. (a) The simulated effective atomic absorption cross section $\sigma(\omega)$ (in a.u.) as a function of the time delay and the photon energy. The extracted pulse (EP) compared to the incident SP, extracted from the (b) $2s2p$, (c) $sp_{2,3+}$, and (d) $sp_{2,4+}$ states.

[1] T. Brabec and F. Krausz, Intense few-cycle laser fields: Frontiers of nonlinear optics, Rev. Mod. Phys. **72,** 545 (2000).

[2] F. Krausz and M. Ivanov, Attosecond physics, Rev. Mod. Phys. **81,** 163 (2009).

[3] E. Goulielmakis, Z.-H. Loh, A. Wirth, R. Santra, N. Rohringer, V. S. Yakovlev, S. Zherebtsov, T. Pfeifer, A. M. Azzeer, M. F. Kling, S. R. Leone, and F. Krausz, Real-time observation of valence electron motion, Nature (London) **466,** 739 (2010).

[4] C. Ott, A. Kaldun, L. Argenti, P. Raith, K. Meyer, M. Laux, Y. Zhang, A. Blättermann, S. Hagstotz, T. Ding, R. Heck, J. Madroero, F. Martn, and T. Pfeifer, Reconstruction and control of a time-dependent two-electron wave packet, Nature (London) **516,** 374 (2014).

[5] X. Huang, Q. Zhang, S. Xu, X. Fu, X. Han, W. Cao, and P. Lu, Coulomb focusing in retrapped ioinization with near-circularly polarized laser field, Opt. Express **27,** 38116 (2019).

[6] J. Liang, Y. Zhou, J. Tan, M. He, Q. Ke, Y. Zhao, M. Li, W. Jiang, and P. Lu, Low-energy photoelectron interference structure in attosecond streaking, Opt. Express **27,** 37736 (2019).

[7] F. Krausz and M. I. Stockman, Attosecond metrology: From electron capture to future signal processing, Nat. Photonics **8,** 205 (2014).

[8] J. Chung and A. M. Weiner, Ambiguity of ultrashort pulse shapes retrieved from the intensity autocorrelation and the power spectrum, IEEE J. Sel. Top. Quantum Electron. **7,** 656 (2001).

[9] D. J. Kane and R. Trebino, Characterization of arbitrary femtosecond pulses using frequencyresolved optical gating, IEEE J. Quantum Electron. **29,** 571 (1993).

[10] C. Iaconis and I. A. Walmsley, Spectral phase interferometry for direct electric-field reconstruction of ultrashort optical pulses, Opt. Lett. **23,** 792 (1998).

[11] A. Baltuska, M. S. Pshenichnikov, and D. A. Wiersma, Second-harmonic generation frequency-resolved optical gating in the single-cycle regime, IEEE J. Quantum Electron. **35,** 459 (1999).

[12] J. R. Birge, R. Ell, and F. X. Kärtner, Two-dimensional spectral shearing interferometry for few-cycle pulse characterization, Opt. Lett. **31,** 2063 (2006).

[13] M. Miranda, T. Fordell, C. Arnold, A. L'Huillier, and H. Crespo, Simultaneous compression and characterization of ultrashort laser pulses using chirped mirrors and glass wedges, Opt. Express **20,** 688 (2012).

[14] M. Miranda, C. L. Arnold, T. Fordell, F. Silva, B. Alonso, R. Weigand, A. L'Huillier, and H. Crespo, Characterization of broadband few-cycle laser pulses with the *d*-scan technique, Opt. Express **20,** 18732 (2012).

[15] J. Itatani, F. Quéré, G. L. Yudin, M. Y. Ivanov, F. Krausz, and P. B. Corkum, Attosecond Streak Camera, Phys. Rev. Lett. **88,** 173903 (2002).

[16] E. Goulielmakis, M. Uiberacker, R. Kienberger, A. Baltuska, V. Yakovlev, A. Scrinzi, T. Westerwalbesloh, U. Kleineberg, U. Heinzmann, M. Drescher, and F. Krausz, Direct measurement of light waves, Science **305,** 1267 (2004).

[17] Y. Mairesse and F. Quéré, Frequency-resolved optical gating for complete reconstruction of attosecond bursts, Phys. Rev. A **71,** 011401 (2005).

[18] K. T. Kim, C. Zhang, A. D. Shiner, B. E. Schmidt, F. Lgar, D. M. Villeneuve, and P. B. Corkum, Petahertz optical oscilloscope, Nat. Photonics **7,** 958 (2013).

[19] A. S. Wyatt, T. Witting, A. Schiavi, D. Fabris, P. Matia-Hernando, I. A. Walmsley, J. P. Marangos, and J. W. G. Tisch, Attosecond sampling of arbitrary optical waveforms, Optica **3,** 303 (2016).

[20] P. Carpeggiani, M. Reduzzi, A. Comby, H. Ahmadi, S. Khn, F. Calegari, M. Nisoli, F. Frassetto, L. Poletto, D. Hoff, J. Ullrich, C. D. Schrter, R. Moshammer, G. G. Paulus, and G. Sansone, Vectorial optical field reconstruction by attosecond spatial interferometry, Nat. Photonics **11,** 383 (2017).

[21] Z. Yang, W. Cao, X. Chen, J. Zhang, Y. Mo, H. Xu, K. Mi, Q. Zhang, P. Lan, and P. Lu, All-optical frequency resolved optical gating for isolated attosecond pulse reconstruction, Opt. Lett. 45, 567 (2020).

[22] M. Geissler, G. Tempea, A. Scrinzi, M. Schnürer, F. Krausz, and T. Brabec, Light Propagation in Field-Ionizing Media: Extreme Nonlinear Optics, Phys. Rev. Lett. **83,** 2930 (1999).

[23] M. B. Gaarde and K. J. Schafer, Generating single attosecond pulses via spatial filtering, Opt. Lett. **31,** 3188 (2006).

[24] S. H. Autler and C. H. Townes, Stark effect in rapidly varying fields, Phys. Rev. **100,** 703 (1955).

[25] N. B. Delone and V. P. Krainov, AC Stark shift of atomic energy levels, Sov. Phys. Usp. **42,** 669 (1999).

[26] M. Chini, B. Zhao, H. Wang, Y. Cheng, S. X. Hu, and Z. Chang, Subcycle ac Stark Shift of Helium Excited States Probed with Isolated Attosecond Pulses, Phys. Rev. Lett. **109,** 073601 (2012).

[27] See the Supplemental Material at http://link.aps.org/supplemental/10.1103/PhysRevApplied.13.014032 for more details about the analytical derivation of the energy shift caused by the signal, the few-level model for AT-splitting simulation, the TDSE model for the perturbed ac Stark shift, waveform sampling using an attosecond pulse train, samplings of the complex electric field structure, samplings of the complex temporal phase, and sampling by means of using a CEP-unstabilized laser.

[28] B. H. Bransden and C. J. Joachain, *Physics of Atoms and Molecules* (Pearson, Harlow, 2003), 2nd ed., Chap. 9.

[29] M. B. Gaarde, C. Buth, J. L. Tate, and K. J. Schafer, Transient absorption and reshaping of ultrafast XUV light by laser-dressed helium, Phys. Rev. A **83,** 013419 (2011).

[30] M. Wu, S. Chen, S. Camp, K. J. Schafer, and M. B. Gaarde, Theory of strong-field attosecond transient absorption, J. Phys. B **49,** 062003 (2016).

[31] C. Ott, A. Kaldun, P. Raith, K. Meyer, M. Laux, J. Evers, C. H. Keitel, C. H. Greene, and T. Pfeifer, Lorentz meets Fano in spectral line shapes: A universal phase and its laser control, Science **340,** 716 (2013).

[32] S. Chen, M. Wu, M. B. Gaarde, and K. J. Schafer, Laser-imposed phase in resonant absorption of an isolated attosecond pulse, Phys. Rev. A **88,** 033409 (2013).

[33] S. Chen, M. Wu, M. B. Gaarde, and K. J. Schafer, Quantum interference in attosecond transient absorption of laser-dressed helium atoms, Phys. Rev. A **87,** 033408 (2013).

[34] M. Chini, X. Wang, Y. Cheng, and Z. Chang, Resonance effects and quantum beats in attosecond transient absorption of helium, J. Phys. B **47,** 124009 (2014).

[35] P. B. Corkum, Plasma Perspective on Strong Field Multiphoton Ionization, Phys. Rev. Lett. **71,** 1994 (1993).

[36] M. Lewenstein, P. Balcou, M. Y. Ivanov, A. L'Huillier, and P. B. Corkum, Theory of high-harmonic generation by low-frequency laser fields, Phys. Rev. A **49,** 2117 (1994).

[37] T. Wittmann, B. Horvath, W. Helml, M. G. Schätzel, X. Gu, A. L. Cavalieri, G. G. Paulus, and R. Kienberger, Single-shot carrier-envelope phase measurement of few-cycle laser pulses, Nat. Phys. **5**, 357 (2009).

[38] D. G. Lappas and A. L'Huillier, Generation of attosecond xuv pulses in strong laser-atom interactions, Phys. Rev. A **58**, 4140 (1998).

[39] W. Cao, P. Lu, P. Lan, X. Wang, and G. Yang, Single-attosecond pulse generation with an intense multicycle driving pulse, Phys. Rev. A **74**, 063821 (2006).

[40] Z. Q. Yang, D. F. Ye, T. Ding, T. Pfeifer, and L. B. Fu, Attosecond XUV absorption spectroscopy of doubly excited states in helium atoms dressed by a time-delayed femtosecond infrared laser, Phys. Rev. A **91**, 013414 (2015).

[41] W. Cao, E. R. Warrick, A. Fidler, D. M. Neumark, and S. R. Leone, Noncollinear wave mixing of attosecond XUV and few-cycle optical laser pulses in gas-phase atoms: Toward multidimensional spectroscopy involving XUV excitations, Phys. Rev. A **94**, 053846 (2016).